Cell, Vol. 88, 265–275, January 24, 1997, Copyright ©1997 by Cell Press

Association of BRCA1 with Rad51 in Mitotic and Meiotic Cells

Ralph Scully,* Junjie Chen,*§ Annemieke Plug,†§ Yonghong Xiao,* David Weaver,* Jean Feunteun,‡ Terry Ashley,† and David M. Livingston*

*The Dana-Farber Cancer Institute
Harvard Medical School
Boston, Massachusetts 02115

†Department of Genetics
Yale University School of Medicine
New Haven, Connecticut 06520–8005

‡Centre National de la Recherche Scientifique
Institut Gustave-Roussy
Cedex 94805 Villejuif
France

Summary

BRCA1 immunostaining reveals discrete, nuclear foci during S phase of the cell cycle. Human Rad51, a homolog of bacterial RecA, behaves similarly. The two proteins were found to colocalize in vivo and to coimmunoprecipitate. BRCA1 residues 758–1064 alone formed Rad51-containing complexes in vitro. Rad51 is also specifically associated with developing synaptonemal complexes in meiotic cells, and BRCA1 and Rad51 were both detected on asynapsed (axial) elements of human synaptonemal complexes. These findings suggest a functional interaction between BRCA1 and Rad51 in the meiotic and mitotic cell cycles, which, in turn, suggests a role for BRCA1 in the control of recombination and of genome integrity.

Introduction

Between 5% and 10% of all breast cancers and 10% of ovarian cancers can be attributed to mutations of highly penetrant, autosomal dominant susceptibility genes (Newman et al., 1988; Claus et al., 1991). One of these is *BRCA1*, which maps to 17q21 (Hall et al., 1990; Narod et al., 1991; reviewed in Feunteun and Lenoir, 1996). *BRCA1* mutations are responsible for almost all families with inherited breast and ovarian cancer and for approximately half of the families with breast cancer only (Easton et al., 1993). The detection of LOH affecting the wild-type *BRCA1* allele in tumors from *BRCA1* mutation carriers implies that *BRCA1* is a tumor suppressor gene (Smith et al., 1992; Neuhausen and Marshall, 1994).

The *BRCA1* cDNA encodes an 1863 residue polypeptide of as yet unknown biochemical function (Miki et al., 1994). The BRCA1 sequence includes an N-terminal RING domain (reviewed in Freemont, 1993; Saurin et al., 1996), a negatively charged region in its C terminus, and C-terminal sequences partially homologous to yeast RAD9 and to a cloned p53 binding protein (Koonin et al., 1996). The negatively charged segment may contribute to transcription-inducing activity of a GAL4–BRCA1 fusion protein (Chapman and Verma, 1996; Monteiro et al., 1996). Whether BRCA1 enacts a transcriptional control function is not yet known.

To date, more than 100 unique, naturally occurring *BRCA1* germline mutations have been identified (Castilla et al., 1994; Friedman et al., 1994; Simard et al., 1994; Shattuck-Eidens et al., 1995). Somatic *BRCA1* mutations have not been detected in sporadic breast cancer and are rare in sporadic ovarian cancer (Merajver et al., 1995). Approximately 90% of breast or ovarian cancer–linked *BRCA1* mutations leads to truncated products. The pattern of truncations and missense mutations suggests that multiple regions of the protein structure contribute to its tumor suppression function.

Multiple BRCA1-specific antibodies detect a protein migrating at ~220 kDa in various cell lines (Chen et al., 1995; Scully et al., 1996). This polypeptide comigrates with and has a peptide map indistinguishable from that of the 220 kDa clonal BRCA1 in vitro translation product (Chapman and Verma, 1996; Scully and Livingston, unpublished data). Several reports indicate that p220 BRCA1 is a nuclear protein in cultured cells and normal tissues (Chen et al., 1995; Chapman and Verma, 1996; Chen et al., 1996; Scully et al., 1996).

The developmental pattern of murine *BRCA1* expression (Lane et al., 1995; Marquis et al., 1995) and its cell cycle–regulated expression (Gudas et al., 1995; Gudas et al., 1996; Vaughn et al., 1996) suggest a relationship between BRCA1 function and cellular proliferation (e.g., in the mammary gland in response to ovarian hormones). Loss of BRCA1 function is a lethal event during murine embryogenesis (Gowen et al., 1996; Hakem et al., 1996; Liu et al., 1996). Some *BRCA1*$^{-/-}$ embryos revealed an early (~E7.5) proliferation block with elevated levels of p21 mRNA at E4 (Hakem et al., 1996).

There are also reports of growth- and transformation-suppressing behavior, as well as death of cells that acutely overproduce BRCA1 (Holt et al., 1996; Rao et al., 1996; Shao et al., 1996; Wilson et al., 1996). However, these studies do not reveal the mechanism underlying these effects.

We have reported that BRCA1 immunostaining is characterized by a "nuclear dot" pattern (Scully et al., 1996). As suggested by the work of Chen et al. (1996) and as defined below, BRCA1 nuclear dots appear in S phase of the cell cycle. Among nuclear proteins known to be characterized by dot-like staining is human Rad51 (hRad51), a homolog of bacterial RecA. hRad51 nuclear dots also appear in S phase (Tashiro et al., 1996).

hRad51 is a member of a protein family known to mediate DNA strand–exchange functions leading to normal recombination (Kowalczykowski, 1991; Radding, 1991; Sung, 1994; Sung and Robberson, 1995; Baumann et al., 1996). Although yeast, mutated for *RAD51*, cannot perform normal meiotic recombination and double-stranded break repair, they are viable (Shinohara et al., 1992). In contrast, mice bearing homozygous, loss-of-function *RAD51* mutations died early in embryogenesis. Moreover, like *BRCA1*$^{-/-}$ embryos, cells of *RAD51*$^{-/-}$ embryos revealed a proliferation defect, suggesting an

§ These authors contributed equally to this work.

additional role for Rad51 in cell growth control (Lim and Hasty, 1996; Tsuzuki et al., 1996). Here, we report that BRCA1 and hRad51 colocalize in S phase cells, interact physically, and, in keeping with previous reports of the behavior of hRad51 (Ashley et al., 1995; Plug et al., 1996), share common space on the surfaces of zygotene and pachytene meiotic chromosomes. These observations identify a biochemical pathway involving BRCA1 and suggest that BRCA1 participates in nuclear processes that lead to normal chromosomal recombination and genome integrity control.

Results

S Phase Nuclear Dot Pattern of BRCA1

The identification of discrete, nuclear dot–like structures as loci of endogenous BRCA1 protein in multiple cell lines and diploid human fibroblasts has been established previously, using seven different BRCA1 monoclonal antibodies (MAb's) and an affinity-purified BRCA1 polyclonal Ab (Scully et al., 1996). BRCA1 nuclear dots were observed in only a fraction of asynchronous cells. The remaining cells revealed a weaker, more diffuse nuclear signal (data not shown). This suggested that the dot-like staining might be cell cycle–dependent. Serum starvation and synchronous release were used to synchronize populations of the breast cancer cell line, MCF7, which were then subjected to BRCA1 immunostaining. In cultures enriched for S phase cells (t = 24 hr population; see Figure 1), most cells scored positively for BRCA1 nuclear dots, while a G1-enriched population presented weaker and largely diffuse nuclear staining (t = 12 hr; see Figure 1 and see also Chen et al., 1996). Analysis of the same cultures with irrelevant MAb revealed no nuclear staining (Scully et al., 1996; data not shown). These and other results not shown here indicate that the BRCA1 nuclear dot pattern is S phase–specific.

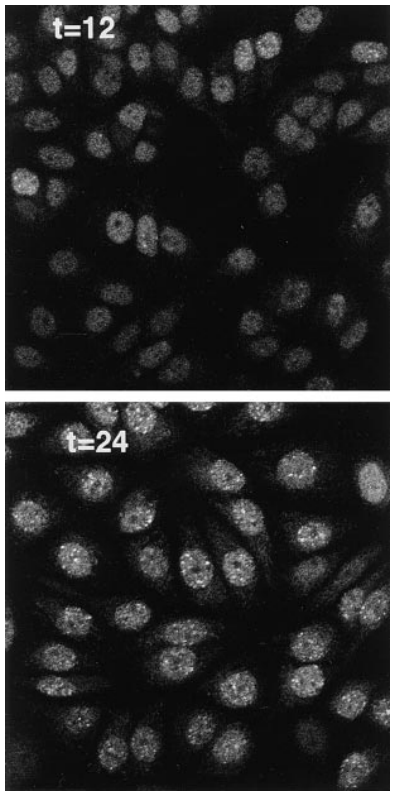

Figure 1. BRCA1 Nuclear Dot Pattern Arises in S Phase

MCF7 cells were serum-starved and released, as described in Experimental Procedures. The figure depicts immunostaining using BRCA1 MAb MS13. Identical results were obtained using two other BRCA1 MAb's (MS110 and AP16). (t = 12), cells 12 hr after serum release (83% G1, 9% S); (t = 24), cells 24 hr after serum release (30% G1, 62% S).

Colocalization of the BRCA1 and Rad51 Immunostaining Patterns in S Phase Nuclei

Rad51, a mammalian RecA homolog, has been shown previously to form S phase–specific nuclear foci (Tashiro et al., 1996). Given the apparent similarity in the timing of appearance of Rad51 and BRCA1 nuclear dots, we asked whether Rad51 and BRCA1 staining colocalize in the same structures. Two-color confocal immunostaining with a BRCA1 monoclonal antibody and an affinity-purified, rabbit polyclonal antiserum raised against clonal human Rad51 (Haaf et al., 1995; Plug et al., 1996) revealed significant, albeit not complete, colocalization of the BRCA1 and the Rad51 nuclear dot patterns (Figure 2). Figure 2 also illustrates cell-to-cell variability in colocalization between BRCA1 and Rad51 signals. In some cells, colocalization of dot signals was extensive (e.g., Figures 2D–2F). In others, the overlap was incomplete (e.g., Figures 2A–2C, top cell). This suggested that the colocalization of BRCA1 and Rad51 is conditional or transient, even in S phase cells. Similar colocalization results were obtained in WI38 and CV-1 cells. These observations raised the possibility that BRCA1 and Rad51 physically interact.

The specificity of the affinity-purified Rad51 antiserum was assessed. Immunoblotting of an MCF7 cell extract with this antiserum revealed a single band, migrating at 38 kDa, the expected size of hRad51 (data not shown). This band disappeared after preabsorbing the antiserum with clonal GST–hRad51 but not with 10-fold more unfused GST. The same was true for the nuclear immunofluorescence signal generated with this Ab. No reaction between this antiserum and authentic BRCA1 was detected by immunoblotting (data not shown).

Biochemical Evidence of an In Vivo BRCA1–Rad51 Interaction

MCF7, 293T, and HeLa cell immunoprecipitates generated with the BRCA1 MAb, SG11, contained endogenous, 38 kDa Rad51, as determined by immunoblotting (Figure 3A and data not shown). The Rad51 and BRCA1 signals detected in SG11 immunoprecipitates were suppressed by preincubation of this BRCA1 antibody with the immunizing BRCA1 peptide. Only a fraction of the ambient Rad51 coimmunoprecipitated with BRCA1 by this method. Although S phase extracts contained more BRCA1–Rad51 complexes than G1 extracts (data not shown), even in S phase–enriched fractions, there was incomplete coprecipitation of hRad51 with BRCA1. Whether this results from the presence of an excess of

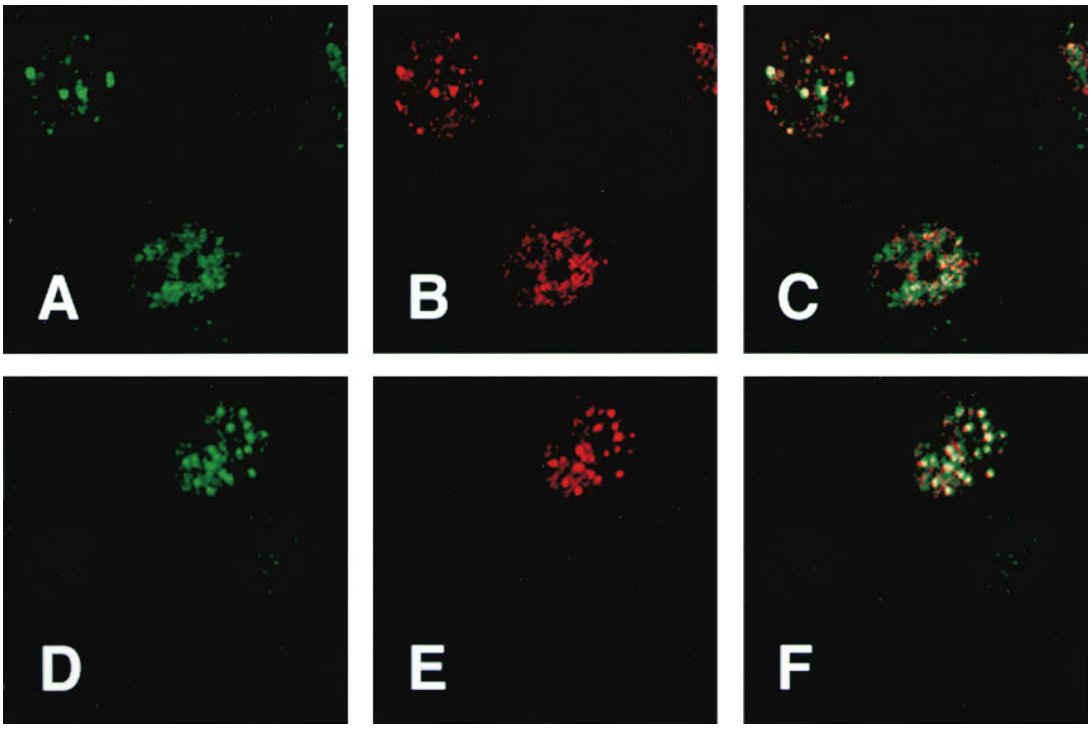

Figure 2. BRCA1 and Rad51 Colocalize in Discrete Nuclear Foci

MCF7 cells were double-stained with BRCA1 MAb MS13 (green) and anti-Rad51 (red). (A) and (D), BRCA1 stain; (B) and (E), Rad51 stain; and (C) and (F), composite BRCA1 and Rad51 stains. Where green and red signals overlap, a yellow pattern is seen, indicating colocalization of BRCA1 and Rad51.

(A–C) Staining of asynchronously growing MCF7 cells, depicting the location of BRCA1 and Rad51 in a BRCA1 dot-containing cell and in a cell exhibiting a more diffuse BRCA1 signal.

(D–E) Staining of serum-starved MCF7 cells, illustrating the rare (5%) S phase cell with a BRCA1 nuclear dot pattern.

Rad51 over BRCA1 and/or only a fraction of Rad51 is competent to bind, directly or indirectly, to BRCA1 is not known.

In an effort to confirm the existence of a physical interaction between BRCA1 and Rad51, we asked whether BRCA1 would complex with epitope-tagged, ectopic Rad51. Figure 3B shows that, after transient transfection of HA-tagged Rad51 into 293T cells, both endogenous BRCA1 and HA-tagged Rad51 were detected in an anti-BRCA1 immunoprecipitate. The coprecipitating band, identified as HA-Rad51, comigrated with bands precipitated from the same extract with either HA or Rad51 antibody. No such band precipitated from untransfected cells with anti-HA MAb (Figure 3B). In addition, transiently overproduced HA–E2F4 was not detected in BRCA1 immunoprecipitates, despite the fact that its concentration was similar to that of HA–Rad51 (data not shown). Hence, the BRCA1 MAb used here did not recognize the HA tag. Moreover, this BRCA1 MAb failed to recognize in vitro translated HA-tagged Rad51 synthesized in a wheat germ extract (data not shown). Hence, it did not appear to recognize Rad51 independently.

In a reciprocal experiment, anti-Rad51 immunoprecipitation of a HA-BRCA1-transfected 293T cell extract coprecipitated BRCA1 (Figure 3C). Despite the presence of higher levels of two HA-tagged control nuclear proteins—the p300 nuclear coactivator and the p130 pocket protein—in parallel transfections of the same cell line, neither protein was detected in anti-Rad51 immunoprecipitates (Figure 3C). Thus, further evidence of specific complex formation between Rad51 and BRCA1 was obtained in transiently transfected cells containing definitively tagged gene products.

BRCA1 Exon 11 Encodes Sequences That Mediate Rad51 Binding

Six overlapping BRCA1 fragments spanning the entire *BRCA1* open reading frame were synthesized as GST fusion proteins (Figures 4A and 4B). Approximately equal amounts of each protein, bound to glutathione-sepharose beads, were incubated with an extract of BJAB (Burkitt's lymphoma–derived) cells. Bead-bound proteins were recovered and separated electrophoretically. The separated proteins were immunoblotted for Rad51 (Figure 4C). GST–BRCA1 fragment #4, corresponding to BRCA1 residues 758–1064, which are encoded by a portion of exon 11, repeatedly bound a 38 kDa immunoreactive Rad51 comigrating band. Identical results were obtained using cell lines MCF7, 293T, and U2OS.

To distinguish between bona fide hRad51 and a comigrating 38 kDa band supplied by the bacterial extract, the same experiment was performed with an extract of ^{35}S-methionine-labeled MCF7 cells (Figure 4D). After incubation of the various bead-bound GST proteins with

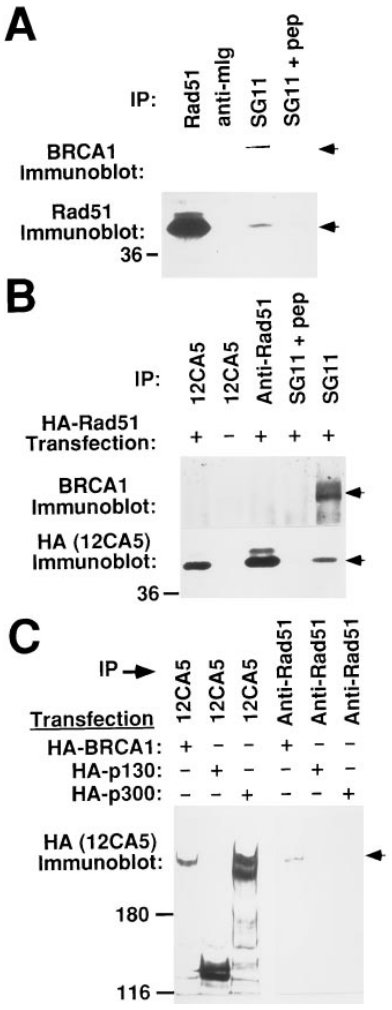

Figure 3. Coimmunoprecipitation of BRCA1 and Rad51

(A) Association in untransfected cells. MCF7 cultures were enriched for S phase (see Experimental Procedures). Extracts (5×10^6 cells per lane) were immunoprecipitated with the antibodies shown. Immunoprecipitated proteins were separated by SDS–PAGE and immunoblotted with MAb MS110 (anti-BRCA1, upper panel; arrow signals the migration position of p220 BRCA1 [Scully et al., 1996]) and with the Rad51 antiserum (arrow signals the presence of the 38 kDa protein). Control antibodies included the rabbit anti-mouse IgG secondary immunoprecipitation antibody ("anti-mIg") and MAb SG11 that had been preincubated with a 10-fold molar excess of the peptide against which it was raised.

(B) Coimmunoprecipitation of ectopic, HA-tagged Rad51 with BRCA1. 293T cells were transfected with an HA-Rad51 expression plasmid. Extracts of the transfected cultures ($\sim 10^7$ cells per lane) were subjected to immunoprecipitation 48 hr later. After SDS–PAGE, immunoblotting for p220 BRCA1 (using MAb MS110, upper panel) and for the HA tag (using MAb 12CA5, lower panel) was performed. Immunoblots of whole cell extracts clearly showed an HA-Rad51-specific doublet migrating at 40–42 kDa (data not shown). The absence of this doublet from an extract of untransfected cells indicated that the 40–42 kDa $12CA5^+$ species depicted in the lower panel are HA–Rad51 products.

(C) Coimmunoprecipitation of ectopic HA-BRCA1 with Rad51. 293T cells were transfected, in parallel, with expression plasmids encoding HA–BRCA1, HA–p130, or HA–p300, as shown. Transfected cell extracts ($\sim 10^7$ cells per lane) were immunoprecipitated. After SDS–PAGE, anti-HA immunoblotting (using MAb 12CA5) was performed. Note that the nominal molecular weights of BRCA1 (220 kDa) and p300 (300 kDa) are not reflected in the relative migration rates of these proteins, which, even in the untagged state, migrate close to one another.

this extract and washing, we eluted the bead-bound proteins. After dilution of the individual eluates to reduce the ambient SDS concentration, the eluted proteins were reimmunoprecipitated with the Rad51 antiserum. A labeled 38 kDa band did reimmunoprecipitate from an eluate of the same lot of GST–BRCA1 #4 fragment-bound beads that yielded the Rad51 immunoreactive band in the earlier experiment (Figure 4C). No such band appeared in the eluates of GST beads alone. Hence, the protein recovered by the BRCA1 #4 fragment is Rad51 and originated in the mammalian and not the bacterial extract.

Taken together, the data indicate that *BRCA1* exon 11 encodes a sequence(s) that can serve as a specific binding site for Rad51. Whether the BRCA1 interaction with Rad51 is direct or depends upon BRCA1 binding to an intermediate protein(s) is not clear at present.

Presence of BRCA1 on Meiotic Chromosomes

The association of BRCA1 and Rad51 in mitotic cells and the known presence of Rad51 on synaptonemal complexes of various organisms (Bishop, 1994; Ashley et al., 1995; Terasawa et al., 1995; Plug et al., 1996) suggested that the two proteins might also colocalize during meiotic prophase. *BRCA1* mRNA is highly expressed in spermatocytes during meiotic prophase (Zabludoff et al., 1996).

The pairing of homologous chromosomes during meiosis is accompanied by the appearance of unique, meiosis-specific DNA- and protein-bearing structures, termed synaptonemal complexes. Following DNA replication in premeiotic S phase, meiotic chromosomes begin to condense and a protein-containing core, or axial element, forms between sister chromatids. As homologous chromosomes synapse in zygonema to form a bivalent, the axial elements align and are joined by transverse filaments. Finally, a discrete central element forms between the two axial elements, completing the structure of the synaptonemal complex. In the current study, we used an antibody to SCP3, a component of the axial/synaptic elements of this structure (Lammers et al., 1994), to visualize the progression of meiotic prophase.

In nuclei of zygotene spermatocytes obtained from fresh, human testis, BRCA1 staining (in red) was observed with three different MAb's (MS13, MS110, and SG11 [Scully et al., 1996]). Chromosomal axes doubly stained with MAb MS110 (red) and Ab to SCP3 (white) are shown in Figure 5. BRCA1 staining was detected in an uneven pattern. On those structures where the specific details of chromosomal anatomy were most clearly discernible, a significant fraction of the staining was noted along unsynapsed axial elements (small arrows, Figure 5A), as well as at axes that were in the process of synapsing (larger arrows, Figure 5A). BRCA1 staining was also detected on unsynapsed centromeric heterochromatin (arrowheads, Figure 5B), on remaining univalents (e.g., small arrow, Figure 5B), and at pairing forks (e.g., larger arrow, Figure 5B). Figure 5D highlights the

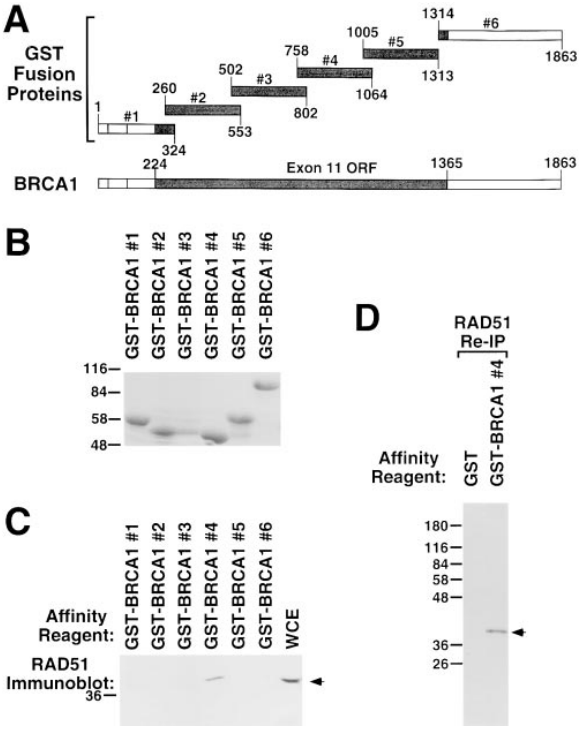

Figure 4. In Vitro Binding of a Segment of BRCA1 to Rad51

Six GST–BRCA1 fusion proteins were generated in E. coli. (A) The schematic diagram of these fusion proteins is not drawn to scale. BRCA1 exon 11 products are indicated by dense stippling. The amino-terminal BRCA1 RING domain is shown by light stippling. BRCA1 residues are marked relative to the translation initiation site.

(B) Synthesis of GST–BRCA1 fusion proteins in E. coli. Individual GST–BRCA1 fusion proteins were prepared as described in Experimental Procedures. The figure depicts a Coomassie blue–stained SDS acrylamide gel, showing the relative abundance of each fusion protein used in Figure 4C. Note that GST–BRCA1 protein #3 was consistently found to be unstable.

(C) Rad51 antiserum recognizes a 38 kDa protein bound to GST–BRCA1 #4. GST–BRCA1 affinity beads were incubated briefly with an unlabeled BJAB extract. After washing, bound proteins were electrophoresed and immunoblotted using the Rad51 antiserum as probe. The figure shows a 38 kDa band, comigrating with Rad51 detected in whole cell extracts (WCE), specifically associated with GST–BRCA1 #4.

(D) The 38 kDa protein bound to GST–BRCA1 #4 is a product of the human cell extract and can be reimmunoprecipitated with Rad51 antiserum. Beads containing GST–BRCA1 #4 and excess GST-containing affinity beads were incubated, in parallel, with extracts of ^{35}S-methionine-labeled MCF7. After washing, bound proteins were solubilized by boiling in SDS buffer. Diluted eluates were then immunoprecipitated with Rad51 antiserum, and the ensuing precipitates were analyzed by SDS–PAGE and autoradiography. The specific 38 kDa band (indicated with an arrow) was found in another experiment to comigrate with the 38 kDa Rad51 protein, as identified by immunoblotting. Furthermore, an anti-Rad51 reimmunoprecipitate from an initial anti-Rad51 precipitate of MCF7 cells yielded only a ^{35}S-labeled 38 kDa species (not shown).

existence of BRCA1 staining on unsynapsed axial elements (small arrows). Arrowheads mark examples of synapsed regions of the indicated synaptonemal complexes. Identical results were obtained with all three BRCA1 Ab's, strongly suggesting that the observed signals resulted from the presence of BRCA1.

Many fewer chromosomes revealed detectable BRCA1 staining in pachynema (Figure 5C). By contrast, BRCA1 staining persisted on the asynapsed X-axis during this period (Figure 5C). Indeed, as pachynema progressed, the BRCA1 signal seemed to be present in a less interrupted manner on late-synapsing autosomal axes (arrows, Figure 5C) and on the X chromosome (see Figure 6), which has no homolog in males. These data imply that the appearance of BRCA1 staining is a synchronous event during meiotic prophase.

The BRCA1 MAb MS13 was raised against a defined segment of the N-terminal region of the cloned protein (residues 1–304, Scully et al., 1996). As another test of specificity, we preincubated MAb MS13, in parallel, with each of two purified BRCA1 fragments. One was the initial MS13 immunogen. The other contained residues 1313–1863. These preincubated preparations were used, in parallel, to stain pachytene spermatocytes. Both Rad51 Ab and a second BRCA1 MAb, MS110, costained the unsynapsed axis of the X chromosome (data not shown). MAb MS13, preincubated with the C-terminal BRCA1 fragment, noted above, also stained the unsynapsed axis of the X chromosome (Figure 6B), which was simultaneously costained with SCP3 Ab (Figure 6A). In contrast, MAb MS13, preincubated with the relevant, immunizing N-terminal polypeptide, yielded no signal despite the presence of the X in that spread (Figures 6C [SCP3 staining] and 6D).

The same experiment was performed with MAb MS110 (which, like MS13, was raised against BRCA1 residues 1–304) with identical results (data not shown). MAb SG11, a third BRCA1 monoclonal Ab, led to a staining pattern identical to that of MS13 and MS110. However, as predicted, SG11 staining was blocked by preincubation with a C-terminal BRCA1 polypeptide containing the SG11 epitope (data not shown). Therefore, the immunostaining obtained with these MAb's likely reflects specific interactions of these MAb's with BRCA1.

A further indication of the specifity of the BRCA1 staining pattern is given by the failure of monoclonal antibodies specific to other nuclear proteins, such as the retinoblastoma protein and the nuclear coactivator, p300, to elicit any signal on human synaptonemal complexes. Furthermore, testis spreads, prepared in this manner, stained positively for DNA (with DAPI) throughout the nucleus. In S phase spermatocytes, nuclei also stained with Ab to the replication protein, RPA, throughout, indicating that the method of preparation does not extract non-SC-bound proteins from the spreads (A. Plug and T. Ashley, unpublished data). The unsynapsed/axial elements, therefore, appear to be the only sites of BRCA1 concentration in zygotene and pachytene spermatocytes.

Simultaneous BRCA1 and Rad51 Staining of Meiotic Chromosomes

Plug et al. (1996) showed that Rad51 is present in premeiotic S phase nuclear foci. During zygonema, Rad51 staining organizes into discrete structures along axial elements. Homologous synapsis is completed in early pachynema, and Rad51 foci remain evident along the

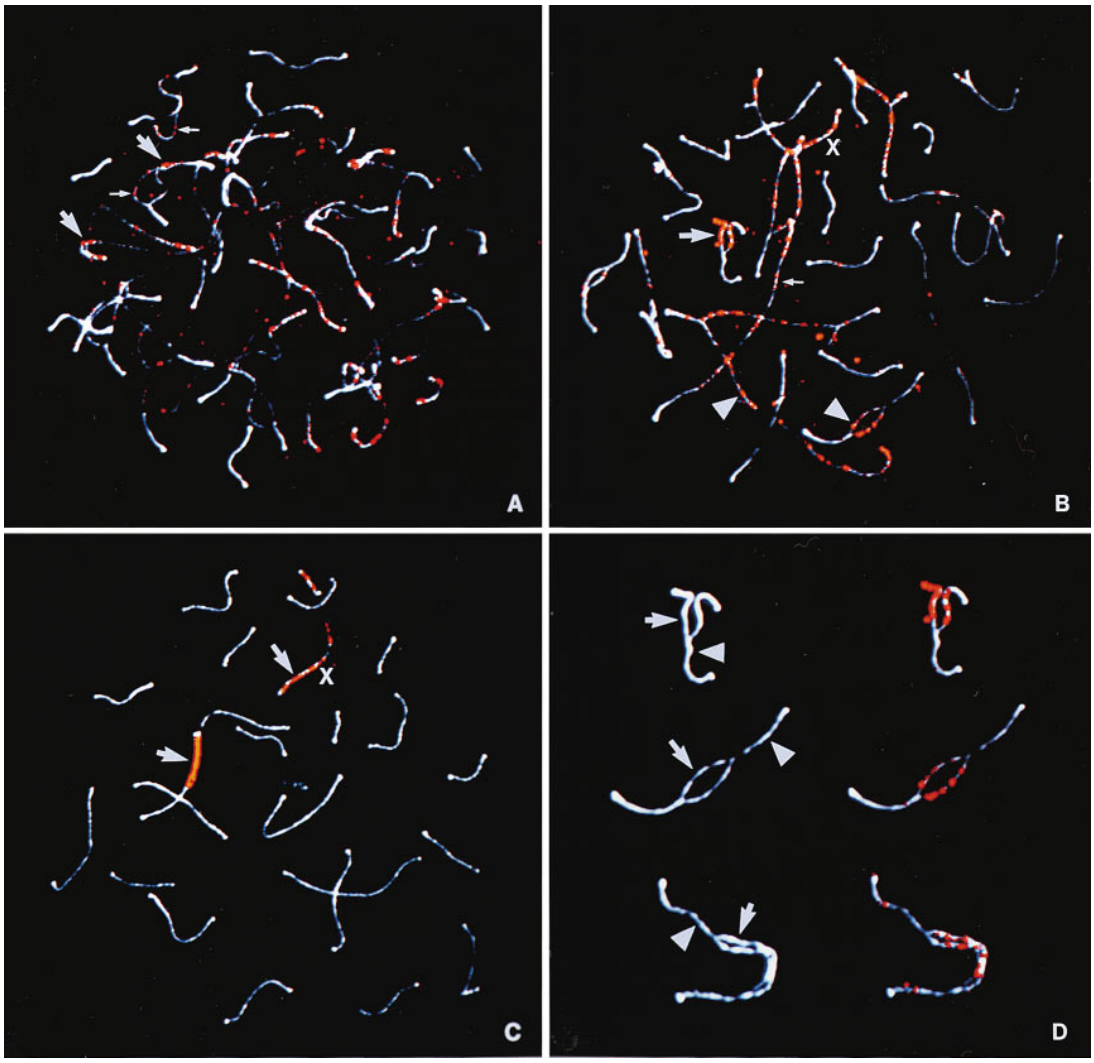

Figure 5. Localization of BRCA1 Staining to Meiotic Chromosomes

(A) Axial and synapsed segments (using Ab SCP3, white) in a human zygotene nucleus. BRCA1 (stained with MAb MS110, red) localized to discrete sites along unsynapsed axial elements (examples noted by small arrows) and axes that are in the process of synapsing (examples noted by larger arrows).

(B) Localization of BRCA1 to sites along unsynapsed axes of regions delayed in synapsis (examples noted by arrowheads), pairing forks (example noted by arrow), and remaining univalents (examples noted by small arrows).

(C) Pachytene nucleus showing the presence of BRCA1 staining on the unsynapsed X chromosome and a delayed pairing fork (arrows).

(D) BRCA1 staining on unsynapsed axial elements (enlarged images taken, in part, from [B]). Arrows indicate examples of unsynapsed segments; arrowheads indicate examples of synapsed regions. SCP3 staining (white) is shown on the left; SCP3 and BRCA 1 costaining (white and red, respectively) are shown on the right. The lowermost complexes of the three are from another zygotene spread, where BRCA1 staining was obtained with MS13.

length of the synaptonemal complex. Shortly after completion of synapsis of most chromosomes, Rad51 foci begin to disappear from the synaptonemal complex. In contrast, Rad51 foci remain associated with the unsynapsed axial element of the X chromosome in spermatocytes (Ashley et al., 1995; Plug et al., 1996). Rad51 foci also remain associated with a few autosomal axes in which synapsis is delayed (Plug et al., unpublished data). In coimmunostaining experiments, much of the BRCA1 staining (red, Figure 7B) and much, albeit not all, of the Rad51 staining (green, Figure 7A; composite image, Figure 7C) appeared in the same general locations on developing synaptonemal complexes during zygonema. In multiple spreads, some foci of Rad51 staining were not associated with a BRCA1 signal at all (Figure 7 and data not shown). One interpretation of the Rad51 and BRCA1 staining patterns, described above, is that a significant fraction of both the BRCA1 and the Rad51 staining, i.e., that which appears in the same general chromosomal locations, is concentrated at unsynapsed chromosomal sites.

Discussion

The data presented here show, for the first time, that BRCA1 associates with Rad51, a human homolog of

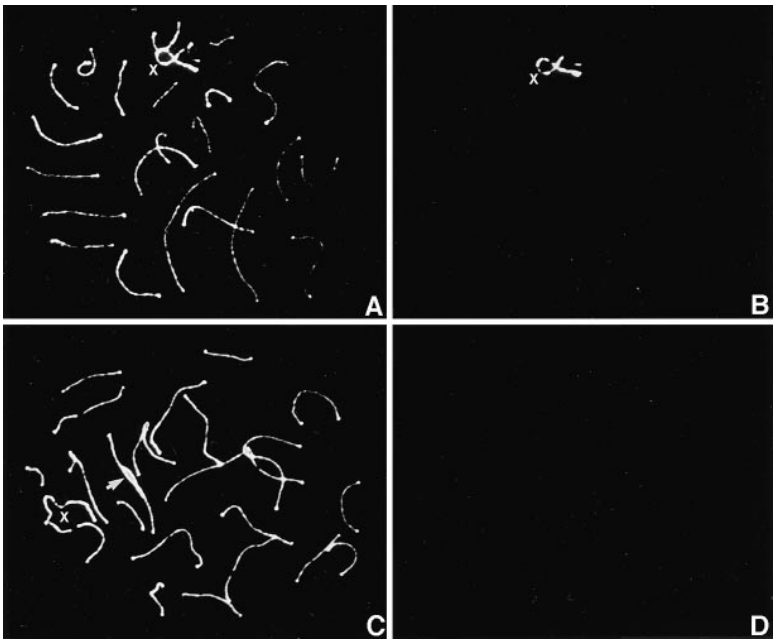

Figure 6. Specificity of BRCA1 Staining of Synaptonemal Complexes

(A) SCP3 staining of pachytene chromosomes.

(B) BRCA1 costaining of this spread with MAb MS13 that had been preincubated with a C-terminal GST–BRCA1 fusion protein, which lacks the MS13 epitope. BRCA1 staining is limited to the unsynapsed axes of the X chromosome.

(C) SCP3 staining of pachytene chromosomes. A prominent X-chromosomal axis is present.

(D) The same spread costained with MS13 preincubated with an N-terminal GST–BRCA1 fusion protein that contains the MS13 epitope.

bacterial RecA. In mitotic cells, this association was marked by colocalization in S phase nuclear foci and coimmunoprecipitation. Furthermore, during meiotic prophase in primary human spermatocytes, the proteins occupied the same general regions of developing synaptonemal complexes. These findings suggest a functional relationship between these two proteins. This conclusion was strengthened by the mapping of a Rad51 interaction domain to BRCA1 residues 758–1064, the site of at least one naturally occurring, loss-of-function missense mutation (Shattuck-Eidens et al., 1995).

Like Rad51, BRCA1 was detected in the nuclei of human spermatocytes on the axial (unsynapsed) elements of developing synaptonemal complexes. This is consistent with the prior observation that *BRCA1* mRNA levels are greatly elevated in zygotene/pachytene spermatocytes (Zabludoff et al., 1996). Since recombination, per se, occurs in synapsed regions, one might speculate that BRCA1 does not act directly in meiotic crossing-over. If that were true, it is possible that BRCA1 acts prior to the initiation of recombination, e.g., as an upstream regulator of this process. Alternatively, since its association with meiotic structures developed and ended synchronously, one could argue that it functions only when it is detected on the meiotic chromosome, e.g., during a period when the search for homologous sequences initiates and proceeds and/or when double-strand breaks appear (reviewed in Kleckner, 1996). The relatively synchronous manner in which BRCA1 appeared on meiotic chromosomes and formed dot structures in mitotic cells suggests a role in both mitotic and meiotic cell cycle control.

Recently, the *ATR* and *ATM* gene products were detected on mutually exclusive regions of the synaptonemal complex (Keegan et al., 1996). Like BRCA1, Atr was found on axial elements, together with Rad51. Atm, the product of another gene whose germ line inactivation may predispose to breast cancer (Swift et al., 1987), was present on synapsed regions. Atr is a homolog of Mec-1 (S. cerevisiae), Rad3 (S. pombe), and mei-41 (Drosophila), and mutations affecting these proteins lead to defects in DNA damage–induced cell cycle responses, radiation hypersensitivity, and defective meiosis (Al-Khodairy and Carr, 1992; Jiminez et al., 1992; Rowley et al., 1992; Cimprich et al., 1996). These large proteins are protein kinases, and, where studied, kinase function was essential to their normal biological activity (Bentley et al., 1996). This, in turn, suggests a role for these proteins in one or more signal transduction cascades, one product of which is proper meiotic and mitotic checkpoint control (reviewed in Carr, 1996).

The question of whether BRCA1 and Atr interact is now clearly relevant. Their similar locations on meiotic chromosomes, the known contribution of Atr to DNA damage control, and its possible role in meiotic cell cycle regulation (Keegan et al., 1996) suggest a related role for BRCA1. The Atr equivalent function in mitotic cells could be monitoring intersister chromatid interactions during S and G2 (Kleckner, 1996). One wonders, then, whether Atr and, possibly, BRCA1 participate in monitoring the progress of DNA replication and/or normal recombination-linked functions.

Tumorigenesis can arise from defects in DNA repair, e.g., in the case of hereditary nonpolyposis colon cancer. There, the defects lie in certain mismatch repair genes (reviewed in Kolodner, 1996). The products of some of these genes are also present on synaptonemal complexes and participate in normal meiosis (Baker et al., 1995; Baker et al., 1996; Edelmann et al., 1996). That BRCA1 and the product(s) of a second class of tumor suppressor genes that play a role in maintaining genome integrity are intimately associated with synaptonemal complexes raises the question of whether they communicate with one another.

What might be the outcome of a specific BRCA1 interaction with Rad51? In yeast, Rad51 participates in double-stranded break repair and meiotic recombination

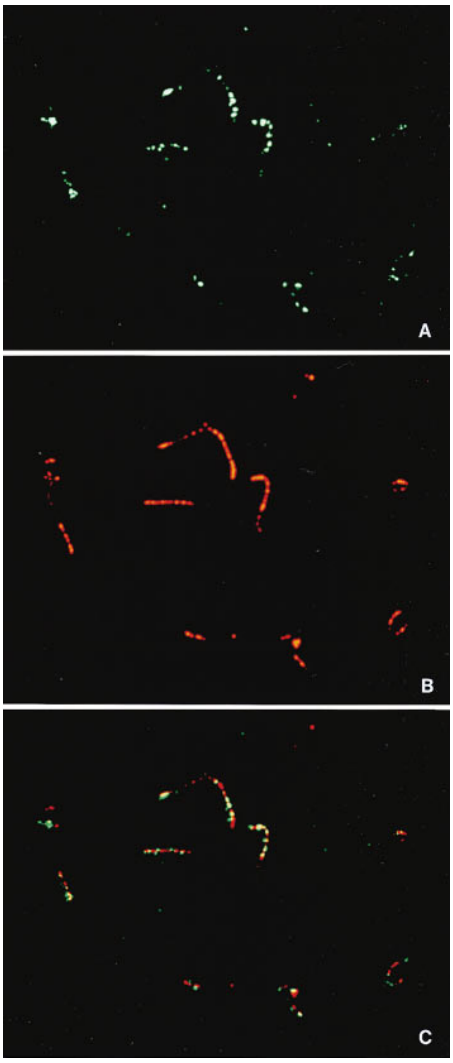

Figure 7. Colocalization of BRCA1 and Rad51 on Meiotic Chromosomes

(A) Rad51 immunostaining (green).

(B) BRCA1 immunostaining (red, MS13).

(C) Rad51 and BRCA1 costaining (colocalization is reflected by yellow images).

(Shinohara et al., 1992). Indeed, it must also play some role in the normal replication of mammalian embryonic cells, since *Rad51*$^{-/-}$ murine zygotes undergo early replication arrest (Lim and Hasty, 1996; Tsuzuki et al., 1996). Finally, RecA function is essential for the SOS response, a bacterial DNA damage control pathway dependent upon the activated transcription of certain genes (reviewed in Echols and Goodman, 1991).

Given these facts, one outcome of the Rad51–BRCA1 interaction could be orderly cell cycle progression, high fidelity DNA replication, and/or events that lead to the maintenance of genomic integrity. Indeed, BRCA1 breast tumors are characterized by a greater degree of genome plasticity than those arising in patients with mutations in the *BRCA2* gene (Marcus et al., 1996). Similarly, given the essential role of RecA in the SOS response and the apparent transcription activation function of certain BRCA1 fusion proteins (Chapman and Verma, 1996; Monteiro et al., 1996), one wonders whether BRCA1 plays a role in mediating a response to mammalian DNA damage in a Rad51/transcription–dependent manner. Notable in this regard is the finding of Reinberg and his coworkers of hRad51 in a fraction of RNA polymerase II holoenzyme (Maldonado et al., 1996).

Importantly, Rad51 and p53, another tumor suppressor with a central role in the response to DNA damage, interact, specifically, in vivo (Sturzbecher et al., 1996). There is a putative p53 interaction sequence in BRCA1 (Koonin et al., 1996) that is distinct from the apparent Rad51 interacting region of BRCA1. p53 also serves as an hereditary breast cancer–inducing gene in patients with the Li-Fraumeni Syndrome (Malkin et al., 1990).

On the face of it, the phenotype (i.e., cell cycle arrest) of *BRCA1* knockout embryos would seem to run counter to a proposed tumor suppressing role for this protein. On the other hand, if BRCA1 has a role in the maintenance of genome integrity, loss of its function might result in genome errors and the subsequent activation of checkpoint genome guardian functions, the outcome of which might be cell cycle arrest. Perhaps only those cells that are already defective in monitoring genome integrity and/or responding to a defect therein can escape the proliferation defect of BRCA1 loss. If this is the case, then loss of BRCA1 function, per se, may not initiate tumorigenesis, but rather accelerate its progression in cells that have already sustained damage to such a checkpoint function.

Interestingly, only trophoblast cells of *BRCA1* knockout embryos developed normally (Hakem et al., 1996). This tissue is unusual in that it normally undergoes endoreplication. If BRCA1 loss trips a normal S phase checkpoint, these cells may not be susceptible to it.

Rad51 loss is lethal in mice but not in yeast, a unicellular organism that may not be subjected to all of the same checkpoint and cell cycle controls as multicellular organisms. Interestingly, yeast also lack a *BRCA1* gene.

Experimental Procedures

Tissue Culture Methods and Preparation of Cell Extracts

Cells were cultured in DMEM-10% fetal bovine serum (FBS), or 10% Fetal Clone I (Hyclone labs). For synchronization studies of MCF7 cells, asynchronous cultures were cultivated for 24 hr in DMEM/0.05% BSA to induce G1 arrest. After release into 20% FBS, cell cycle progression was measured by FACS analysis. Maximum S phase enrichment was seen 24 hr after serum release. For transfection, a standard calcium phosphate precipitation method was used (Wigler et al., 1977). Immunoprecipitation (typically ~2 μg Ab per reaction) and immunoblotting were performed as described previously (Scully et al., 1996), with the exception of the extraction buffer, which contained only NP-40 (0.5%) as detergent.

Immunostaining of Adherent Cells

Cells were fixed and permeablized as described previously (Eckner et al., 1994). Primary antibodies were incubated in a humidified atmosphere at 37°C for 20 min. Species-specific, fluorochrome-conjugated secondary antibodies (Jackson Immunoresearch) were incubated in a similar fashion. Immunofluorescence was recorded using a Zeiss confocal microscope.

Preparation and Immunostaining of Human Synaptonemal Complexes

Preparation of "spreads" of human spermatocytes was perfomed as described by Peters et al. (1997). Antibody incubation and detection

were performed as described previously (Moens et al., 1987; Ashley et al., 1995). BRCA1 MAb's were detected with anti-mouse IgG rhodamine conjugate (Pierce), and SCP3 polyclonal antibodies with anti-rabbit IgG FITC conjugate (Pierce). Preparations were counterstained with 4′,6′ diamino-2-phenylindole (DAPI, Sigma), mounted in a DABCO (Sigma) antifade solution, and examined on a Zeiss Axioskop (63-X and 100-X, 1.2 Plan Neofluor oil immersion objective). Each fluorochrome image was captured separately as an 8-bit source image using a computer-assisted cooled CCD camera (Photometrics CH 220). The separate images were 24-bit pseudocolored and merged with custom software developed by Tim Rand (Ried et al., 1992).

Construction of *BRCA1* and *Rad51* Expression Vectors

To optimize in vivo expression of *BRCA1* cDNA, a rabbit β-globin intron was inserted into pcDNA3 (Invitrogen). The insert was generated by PCR from vector pSG5 (Stratagene), using the primers: 5′-GGGCCAAGCTTGCGTCTAGAGTCGATCCTGAGAACTTCAG GGTG-3′ and 5′-GGGGGATCCGCCCGGGCCAAGCTTGGGGTCGA CAGCACAATAACCAGCACGTTGCCC-3′. The pcDNA3 HindIII restriction site was converted to a unique NheI site using HindIII digestion, Klenow treatment, and religation. The insert was digested with XbaI and BamHI and subcloned into the NheI–BamHI sites of pcDNA3. Full sequencing of the insert showed that nucleotides AATAA (underlined above) had been replaced by the sequence AAA. No other errors were found. This vector was termed "pcDNA3β."

Derivation of the wild-type human cDNA for BRCA1 has been described previously (Scully et al., 1996). An amino-terminal HA–BRCA1 expression vector was generated by PCR of BRCA1 cDNA (using primers 5′-GGGGGATCCATGGATTTATCTGCTCTTCGCG-3′ and 5′-GGGTCAGAATTCAGCCTTTTCTACATTCATTCTGTC-3′). A BamHI–BstXI fragment of this product was subcloned into the same sites of a partial *BRCA1* cDNA, and the full-length cDNA was reassembled into pcDNA3β containing a previously subcloned HA tagcoding sequence (Krek et al., 1993) located between HindIII and BamHI sites. The PCR-derived part was confirmed correct by direct sequencing.

An amino-terminal HA-tagged *hRad51* expression construct was generated in a similar fashion. A full-length *hRad51* cDNA, housing a BamHI site immediately upstream of the open reading frame, was generated by using Pfu polymerase and PCR primers: 5′-GGG CCCGGATCCATGGCAATGCAGATGCAGC-3′ and 5′-GGGCCCCAA TTGGATATCATTCAGTCTTTGGCATCTCCCACTCC-3′. Restriction digests confirmed the identity of the cloned fragment, which was subcloned into BamHI–EcoRV sites of a pcDNA3/HA vector, as described above. Expression vectors for HA-p300 and HA-p130 have been described previously (Eckner et al., 1994; Vairo et al., 1995).

Construction and Expression of Bacterial GST-Fusion Proteins

Constructs corresponding to GST–BRCA1 #1–#5 (see text) were made using the vector pGEX-5X3 (Pharmacia). Inserts were generated by PCR using Pfu polymerase and the following pairs of primers: (#1) 5′-ATAGGATCCAAATGGATTTATCTGCTCTTCGC-3′ and 5′-ATAGTCGACTTCCAGCCCATCTGTTATGT-3′; (#2) 5′-ATAGGAT CCAGGGTAGTTCTGTTTCAAACTTG-3′ and 5′-ATAGTCGACCACT ATTAGTAATATTCATCACT-3′; (#3) 5′-ATAGGATCCGTAAAAGGAG ACCTACATCAG-3′ and 5′-ATAGTCGACTCACACATTTATTTGGTT CTG-3′; (#4) 5′-ATAGGATCCAAACTGAAAGATCTGTAGAGAGT-3′ and 5′-ATAGTCGACTGGAACCTATTTCATTAATAC-3′; and (#5) 5′-ATAGGATCCCATTCAATGTCACCTGAAAGA-3′ and 5′-ATAGTCGA CTGGGTGTTTGTATTTGCAGTCAA-3′.

GST–BRCA1 fragment #6 was described previously (Scully et al., 1996). GST–hRad51 was generated using the *Rad51* cDNA described above. Synthesis of GST fusion proteins and their partial purification on glutathione-sepharose beads was performed as described (Kaelin et al., 1992). Where GST fusion proteins were used for specificity controls, they were used as glutathione-eluted protein (10 μg per sample) or as affinity beads.

Acknowledgments

We are especially indebted to Drs. Nancy Kleckner, Bill Kaelin, Jim DeCaprio, Myles Brown, and Richard Kolodner for stimulating and helpful discussions. We are grateful to Drs. Adam Kibel and Jerome Ritchie for their expert help in obtaining testis tissue for these experiments. Drs. Charles Radding, Efim Golub, Gurucharan Reddy, and Oleg Kovalenko generously provided affinity-purified hRad51 antibody, and we thank them enthusiastically for it. We also thank Dr. Christa Heyting for her generosity in supplying SCP3 antibody and Mr. Phillipe Male for processing meiosis photographs. This work was supported by grants from the National Institutes of Health and the Dana-Farber Women's Cancer Program.

Received December 2, 1996; revised December 20, 1996.

References

Al-Khodairy, F., and Carr, A.M. (1992). DNA repair mutants defining G2 checkpoint pathways in Schizosaccharomyces pombe. EMBO J. *11*, 1343–1350.

Ashley, T., Plug, A.W., Xu, J., Solari, A.J., Reddy, G., Golub, E.I., and Ward, D.C. (1995). Dynamic changes in Rad51 distribution on chromatin during meiosis in male and female vertebrates. Chromosoma *104*, 19–28.

Baker, S.M., Bronner, C.E., Zhang, L., Plug, A.W., Robatzek, M., Warren, G., Elliott, E.A., Yu, J., et al. (1995). Male mice defective in the DNA mismatch repair gene PMS2 exhibit abnormal chromosome synapsis in meiosis. Cell *82*, 309–319.

Baker, S.M., Plug, A.W., Prolla, T.A., Bronner, C.E., Harris, A.C., Yao, X., Christie, D.-M., Monell, C., et al. (1996). Involvement of mouse Mlh1 in DNA mismatch repair and meiotic crossing over. Nat. Genet. *13*, 336–342.

Baumann, P., Benson, F.E., and West, S.C. (1996). Human Rad51 protein promotes ATP-dependent homologous pairing and strand transfer reactions in vitro. Cell *87*, 757–766.

Bentley, N.J., Holtzman, D.A., Keegan, K.S., Flaggs, G., DeMaggio, A.J., Ford, J.C., Hoekstra, M.F., and Carr, M. (1996). The Schizosaccharomyces pombe rad3 checkpoint gene. EMBO J., in press.

Bishop, D.K. (1994). RecA homologues Dmc1 and Rad51 interact to form multiple nuclear complexes prior to meiotic chromosome synapsis. Cell *79*, 1081–1092.

Carr, A.M. (1996). Checkpoints take the next step. Science *271*, 314–315.

Castilla, L.H., Couch, F.J., Erdos, M.R., Hoskins, K.F., Calzone, K., and Garber, J.E. (1994). Mutations in the BRCA1 gene in families with early-onset breast and ovarian cancer. Nat. Genet. *8*, 387–391.

Chapman, M.S., and Verma, I.M. (1996). Transcriptional activation by BRCA1. Nature *382*, 678–679.

Chen, Y., Chen, C.-F., Riley, D.J., Allred, D.C., Chen, P.-L., Von Hoff, D., Osborne, C.K., and Lee, W.-H. (1995). Aberrant subcellular localization of BRCA1 in breast cancer. Science *270*, 789–791.

Chen, Y.M., Farmer, A.A., Chen, C.F., Jones, D.C., Chen, P.L., and Lee, W.H. (1996). BRCA1 is a 220-kDa nuclear phosphoprotein that is expressed and phosphorylated in a cell cycle–dependent manner. Cancer Res. *56*, 3168–3172.

Cimprich, K.A., Shin, T.B., Keith, C.T., and Schreiber, S.L. (1996). cDNA cloning and gene mapping of a candidate human cell cycle checkpoint protein. Proc. Natl. Acad. Sci. USA *7*, 2850–2855.

Claus, E.B., Risch, N., and Thompson, W.D. (1991). Genetic analysis of breast cancer in the Cancer and Steroid Hormone Study. Am. J. Hum. Genet. *48*, 232–241.

Easton, D.F., Bishop, T., Ford, D., Crockford, G.P., and The Breast Cancer Linkage Consortium (1993). Genetic linkage analysis in familial breast and ovarian cancer: results from 214 families. Am. J. Hum. Genet. *52*, 678–701.

Echols, H., and Goodman, M.F. (1991). Fidelity mechanisms in DNA replication. Annu. Rev. Biochem. *60*, 477–511.

Eckner, R., Ewen, M.E., Newsome, D., Gerdes, M., DeCaprio, J.A., Lawrence, J.B., and Livingston, D.M. (1994). Molecular cloning and functional analysis of the adenovirus E1A-associated 300-kD protein (p300) reveals a protein with properties of a transcriptional adaptor. Genes Dev. *8*, 869–884.

Edelmann, W., Cohen, P.E., Kane, M., Lau, K., Morrow, B., Bennett, S., Umar, A., Kunkel, T., et al. (1996). Meiotic pachytene arrest in MLH1-deficient mice. Cell *85*, 1125–1134.

Feunteun, J., and Lenoir, G.M. (1996). BRCA1, a gene involved in inherited predisposition to breast and ovarian cancer. Biochem. Biophys. Acta *1242*, 177–180.

Freemont, P.S. (1993). The RING finger. Ann. NY Acad. Sci. *684*, 174–192.

Friedman, L.S., Ostermeyer, E.A., Szabo, C.I., Dowd, P., Lynch, E.D., Rowell, S.E., and King, M.-C. (1994). Confirmation of BRCA1 by analysis of germline mutations linked to breast and ovarian cancer in ten families. Nat. Genet. *8*, 399–404.

Gowen, L.C., Johnson, B.L., Latour, A.M., Sulik, K.K., and Koller, B.H. (1996). BRCA1 deficiency results in early embryonic lethality characterized by neuroepithelial abnormalities. Nat. Genet. *12*, 191–194.

Gudas, J.M., Li, T., Nguyen, H., Jensen, D., Rauscher, F.J.I., and Cowan, K.H. (1996). Cell cycle regulation of BRCA1 messenger RNA in human breast epithelial cells. Cell Growth Differ. *7*, 717–723.

Gudas, J.M., Nguyen, H., Li, T., and Cowan, K. (1995). Hormone-dependent regulation of BRCA1 in human breast cancer cells. Cancer Res. *55*, 4561–4565.

Haaf, T., Golub, E.I., Reddy, G., Radding, C.M., and Ward, D.C. (1995). Nuclear foci of mammalian Rad51 recombination protein in somatic cells after DNA damage and its localization in synaptonemal complexes. Proc. Natl. Acad. Sci. USA *92*, 2298–2302.

Hakem, R., de la Pomba, J.L., Sirard, C., Mo, R., Woo, M., Hakem, A., Wakeham, A., Potter, J., et al. (1996). The tumor suppressor gene *Brca1* is required for embryonic cellular proliferation in the mouse. Cell *85*, 1009–1023.

Hall, J.M., Lee, M.K., and Newmann, B. (1990). Linkage of early-onset breast cancer to chromosome 17q21. Science *250*, 1684–1689.

Holt, J.T., Thompson, M.E., Szabo, C., Robinson-Benion, C., Arteaga, C. L., King, M.-C., and Jensen, R.A. (1996). Growth retardation and tumor inhibition by BRCA1. Nat. Genet. *12*, 298–302.

Jiminez, G., Yucel, J., Rowley, R., and Subramani, S. (1992). The rad3^{+} gene of Schizosaccharomyces pombe is involved in multiple checkpoint functions and in DNA repair. Proc. Natl. Acad. Sci. USA *87*, 4952–4956.

Kaelin, W.G., Jr., Krek, W, Sellers, W.R., DeCaprio, J.A., Ajchenbaum, F., Fuchs, C.S., Chittenden, T., Li, Y., Farnham, P.J., et al. (1992). Expression cloning of a cDNA encoding a retinoblastoma-binding protein with E2F-like properties. Cell *70*, 351–364.

Keegan, K.S., Holtzman, D.A., Plug, A.W., Christenson, E.R., Brainerd, E.E., Flaggs, G., Bentley, N.J., Taylor, E.M., et al. (1996). The Atr and Atm protein kinases associate with different sites along meiotically pairing chromosomes. Genes Dev. *10*, 2423–2437.

Kleckner, N. (1996). Meiosis: how could it work? Proc. Natl. Acad. Sci. USA *93*, 8167–8174.

Kolodner, R. (1996). Biochemistry and genetics of eukaryotic mismatch repair. Genes Dev. *10*, 1433–1442.

Koonin, V.F., Altschul, S.F., and Bork, P. (1996). BRCA1 protein products: functional motifs. Nat. Genet. *13*, 266–267.

Kowalczykowski, S.C. (1991). Biochemistry of genetic recombination: energetics and mechanism of DNA strand exchange. Annu. Rev. Biophys. Chem. *20*, 539–575.

Krek, W., Livingston, D.M., and Shirodkar, S. (1993). Binding to DNA and the retinoblastoma gene product promoted by complex formation of different E2F family members. Science *262*, 1557–1560.

Lammers, J.H.M., Offenberg, H.H., van Aalderen, M., Vink, A.C., Dietrich, A.J., and Heyting, C. (1994). The gene encoding a major component of the lateral element of the synaptonemal complex of the rat is related to X-linked lymphocyte-regulated genes. Mol. Cell. Biol. *14*, 1137–1146.

Lane, T.F., Deng, C., Elson, A., Lyu, M.S., Kozak, C.A., and Leder, P. (1995). Expression of BRCA1 is associated with terminal differentiation of ectodermally and mesodermally derived tissues in mice. Genes Dev. *9*, 2712–2722.

Lim, D.-S., and Hasty, P. (1996). A mutation in mouse rad51 results in an early embryonic lethal that is suppressed by a p53 mutation. Mol. Cell. Biol. *16*, 7133–7143.

Liu, C.Y., Flesken-Nikitin, A., Li, S., Zeng, Y., and Lee, W.-H. (1996). Inactivation of the mouse Brca1 gene leads to failure in the morphogenesis of the egg cylinder in early postimplantation development. Genes Dev. *10*, 1835–1843.

Maldonado, E., Shiekhattar, R., Sheldon, M., Cho, H., Drapkin, R., Rickert, P., Lees, E., Anderson, C.W., Linn, S., and Reinberg, D. (1996). A human RNA polymerase II complex associated with SRB and DNA-repair proteins. Nature *381*, 86–89.

Malkin, D., Li, F.P., Strong, L.C., Fraumeni, J.F., Jr., Nelson, C.E., Kim, D.H., Kassel, J., Gryka, M.A., Bischoff, F.Z., et al. (1990). Germ line p53 mutations in a familial syndrome of breast cancer, sarcomas, and other neoplasms. Science *250*, 1233–1238.

Marcus, J.N., Watson, P., Page, D.L., Narod, S.A., Lenoir, G., Tonin, P., Linder-Stephenson, L., et al. (1996). Hereditary breast cancer: pathobiology, prognosis, and BRCA1 and BRCA2 gene linkage. Cancer *77*, 697–709.

Marquis, S.T., Rajan, J.V., Wynshaw-Boris, A., Xu, J., and Yin, G.-Y. (1995). The developmental pattern of BRCA1 expression implies a role in differentiation of the breast and other tissues. Nat. Genet. *11*, 17–26.

Merajver, S.D., Pham, T.M., Caduff, R.F., Chen, M., Poy, E.L., Cooney, K.A., Weber, B.L., Collins, F.S., et al. (1995). Somatic mutations in the BRCA1 gene in sporadic ovarian tumors. Nat. Genet. *9*, 439–443.

Miki, Y., Swensen, J., Shattuck-Eidens, D., Futreal, P.A., Harshman, K., Tavtigian, S., Liu, Q., Cochran, C., et al. (1994). A strong candidate for the breast and ovarian cancer susceptibility gene BRCA1. Science *266*, 66–71.

Moens, P.B.C., Heyting, C., Dietrich, A.J., van Raamsdonk, W., and Chen, Q. (1987). Synaptonemal complex antigen localization and conservatation. J. Cell Biol. *105*, 93–103.

Monteiro, A.N.A., August, A., and Hanafusa, H. (1996). Evidence for a transcriptional activation function of BRCA1 C-terminal region. Proc. Natl. Acad. Sci. USA *93*, 13595–13599.

Narod, S.A., Feunteun, J., Lynch, H.T., Watson, P., Conway, T., Lynch, J., and Lenoir, G. (1991). Familial breast-ovarian cancer locus on chromosome 17q12–23. Lancet *338*, 82–83.

Neuhausen, S.L., and Marshall, C.J. (1994). Loss of heterozygosity in familial tumors from three BRCA1-linked kindreds. Cancer Res. *54*, 6069–6072.

Newman, B., Austin, M.A., Lee, M., and King, M.-C. (1988). Inheritance of breast cancer: evidence for autosomal dominant transmission in high risk families. Proc. Natl. Acad. Sci. USA *85*, 1–5.

Peters, A.H.F.M., Plug, A.W., van Vugt, M.J. and deBoer, P. (1997). Drying down method for spreading mammalian meiocytes from the male and female germline. Chromosoma *5*, 1–3.

Plug, A.W., Xu, J., Reddy, G., Golub, E.I., and Ashley, T. (1996). Presynaptic association of Rad51 protein with selected sites in meiotic chromatin. Proc. Natl. Acad. Sci. USA *93*, 5920–5924.

Radding, C.M. (1991). Helical interactions in homologous pairing and strand exchange driven by RecA protein. J. Biol. Chem. *266*, 5355–5358.

Rao, V.N., Shao, N., Ahmad, M., and Reddy, E.S. (1996). Antisense RNA to the putative tumor suppressor gene BRCA1 transforms mouse fibroblasts. Oncogene *12*, 523–528.

Ried, T., Baldini, A., Rand, T.C. and Ward, D.C. (1992). Simultaneous visualization of seven different DNA probes by in situ hybridization using combinatorial fluorescence and digital imaging microscopy. Proc. Natl. Acad. Sci. USA *89*, 1388–1392.

Rowley, R., Subramani, S., and Young, P.G. (1992). Checkpoint controls in Schizosaccharomyces pombe, rad 1. EMBO J. *11*, 1335–1342.

Saurin, A.J., Borden, K.L. B., Boddy, M.N., and Freemont, P.S. (1996). Does this have a familiar RING? Trends Biochem. Sci. *21*, 208–214.

Scully, R., Ganesan, S., Brown, M., De Caprio, J.A., Cannistra, S.A., Feunteun, J., Schnitt, S., and Livingston, D.M. (1996). Location of BRCA1 in human breast and ovarian cell lines. Science *272*, 123–125.

Shao, N.S., Chai, Y.L., Shyam, E., Reddy, P., and Rao, N.V. (1996). Induction of apoptosis by the tumor suppressor protein BRCA1. Oncogene *13*, 1–7.

Shattuck-Eidens, D., McClure, M., Simard, J., Labrie, F., Narod, S., Couch, F., Hoskins, K., Weber, B., et al. (1995). A collaborative survey of 80 mutations in the BRCA1 breast and ovarian cancer susceptibility gene. J. Am. Med. Assoc. *273*, 535–541.

Shinohara, A., Ogawa, H., and Ogawa, T. (1992). Rad51 protein involved in repair and recombination in Saccharomyces cerevisiae is a RecA-like protein. Cell *69*, 457–470.

Simard, J., Tonin, P., Durocher, F., Morgan, K., Rommens, J., and Gingras, S. (1994). Common origins of BRCA1 mutations in Canadian breast and ovarian cancer families. Nat. Genet. *8*, 392–398.

Smith, S.A., Easton, D.F., Evans, D.G.R., and Ponder, B.A.J. (1992). Allele losses in the region 17q12–q21 in familial breast and ovarian cancer non-randomly involve the wild-type chromosome. Nat. Genet. *2*, 128–131.

Sturzbecher, H.-W., Donzelmann, B., Henning, W., Knippschild, U., and Buchop, S. (1996). p53 is linked directly to homologous recombination processes via RAD51/RecA protein interaction. EMBO J. *15*, 1992–2002.

Sung, P. (1994). Catalysis of ATP-dependent homologous DNA pairing and strand exchange by yeast Rad51 protein. Science *265*, 1241–1243.

Sung, P., and Robberson, D.L. (1995). DNA strand exchange mediated by a Rad51–ssDNA nucleoprotein filament with polarity opposite to that of RecA. Cell *82*, 453–461.

Swift, M., Reitnauer, P.J., Morrell, D., and Chase, C.L. (1987). Breast and other cancers in families with Ataxia-Telangiectasia. N. Engl. J. Med. *316*, 1289–1294.

Tashiro, S., Kotomura, N., Shinohara, A., Tanaka, K., Ueda, K., and Kamada, N. (1996). S phase specific formation of the human Rad51 protein nuclear foci in lymphocytes. Oncogene *12*, 2165–2170.

Terasawa, M., Shinohara, A., Hotta, Y., Ogawa, H., and Ogawa, T. (1995). Localization of RecA-like recombination proteins on chromosomes of lily at various meiotic stages. Genes Dev. *9*, 925–934.

Tsuzuki, T., Fujii, Y., Sakumi, K., Tominaga, Y., Nakao, K., Sekiguchi, M., Matsushiro, A., Yoshimura, Y., and Morita, T. (1996). Targeted disruption of the Rad51 gene leads to lethality in embryonic mice. Proc. Natl. Acad. Sci. USA *93*, 6236–6240.

Vairo, G., Livingston, D.M., and Ginsberg, D. (1995). Functional interaction between E2F-4 and p130: evidence for distinct mechanisms underlying growth suppression by different retinoblastoma protein family members. Genes Dev. *9*, 869–881.

Vaughn, J.P., Davis, P.L., Jarboe, M.D., Huper, G., Evans, A.C., Wiseman, R.W., Berchuck, A., Iglehart, J.D., et al. (1996). BRCA1 expression is induced before DNA synthesis in both normal and tumor-derived breast cells. Cell Growth Differ. *7*, 711–715.

Wigler, M., Silverstein, S., Lee, L.S., Pellicer, A., Cheg, Y.C., and Axel, R. (1977). Transfer of purified herpes virus thymidine kinase gene to cultured mouse cells. Cell *11*, 223–232.

Wilson, C.A., Payton, M.N., Elliott, G.S., Buaas, F.W., Cajulis, E.E., Grosshans, D., Ramos, L., Reese, D.M., et al. (1996). Differential subcellular localization, expression and biological toxicity of BRCA1 and the splice variant BRCA1-Δ11b. Oncogene, in press.

Zabludoff, S.D., Wright, W.W., Harshman, K., and Wold, B.J. (1996). BRCA1 mRNA is expressed highly during meiosis and spermiogenesis but not during mitosis of male germ cells. Oncogene *13*, 649–653.